Synthesis of n-dodecylamine borane C12H25NH2BH3, its stability against hydrolysis, and its characterization in THF

Antigoni Theodoratou, Kevin Turani-I-Belloto, Eddy Petit, Sandrine Dourdain, Johan Alauzun, Umit Demirci

Version of Record: https://www.sciencedirect.com/science/article/pii/S0022286021016124
Manuscript_0233d5be456981af692000073f1fdf32

Synthesis of *n*-dodecylamine borane $C_{12}H_{25}NH_2BH_3$, its stability against hydrolysis, and its characterization in THF

Antigoni Theodoratou,[1] Kevin Turani-I-Belloto,[2] Eddy Petit,[2] Sandrine Dourdain,[3] Johan G. Alauzun,[1] Umit B. Demirci [2]*

[1] ICGM, Univ Montpellier, CNRS, ENSCM, Montpellier, France.

[2] Institut Europeen des Membranes, IEM – UMR 5635, Universite de Montpellier, ENSCM, CNRS, 34090 Montpellier, France.

[3] ICSM, Univ Montpellier, CEA, CNRS, ENSCM, Marcoule, France

* *corr. author*: umit.demirci@umontpellier.fr

Abstract

Dihydrogen $H^{\delta+}\cdots H^{\delta-}$ bonding that is accepted as an important unconventional hydrogen bonding could play a key role in molecular self-assembly of amine boranes. It is with this goal in mind that we have studied the behavior of *n*-dodecylamine borane $nC_{12}H_{25}NH_2BH_3$ (C12AB) dissolved in anhydrous THF. C12AB can be easily synthesized with a purity higher than 99% by Lewis acid-base reaction of a BH_3 complex with *n*-dodecylamine $nC_{12}H_{25}NH_2$. It is stable when dissolved in THF that is a good solvent of it. However, it is unstable in the presence of moisture, readily hydrolyzing and producing water-soluble borates. Molecular self-assembly of C12AB has thus to be studied in anhydrous conditions, which allows observing by DLS and SAXS-WAXS the formation of core-shell aggregates in anhydrous THF. The aggregates consist of about five self-assembling stretched C12AB molecules where the NH_2BH_3 groups are in the core of 3 Å and the alkyl chains in an outer-shell.

Keywords

Amine borane; Dihydrogen bonding; Dodecylamine; Hydrolysis; Self-assembly.

1. Introduction

Amine boranes are old compounds. The first to be discovered is ammonia trifluoroborane NH_3BF_3, which was reported in 1809 by Gay-Lussac and Thenard [1]. In 1937, the first amine borane-3h, *N*,*N*,*N*-trimethylamine borane $N(CH_3)_3BH_3$, was reported by Burg and Schlesinger [2]. In 1955, the fully-hydrogenated amine borane, ammonia borane NH_3BH_3 (AB), was reported by Shore and Parry [3]. Nowadays, AB is undoubtedly the best known amine borane. It "has received disproportionately more attention than any other amine borane due to its potential as a hydrogen storage material" [4]. This is still true though other amine boranes have been developed for the same application [5]. A few examples are methylamine borane [6], ethylenediamine borane [7], 1,2-BN cyclohexane [8], and lithium amidoborane [9].

The interest in amine boranes goes beyond the hydrogen storage application. Amine boranes have been used as pharmacologically active substances [10], reagents in organic and organometallic chemistry [11,12], reducing agents [13], monomers of linear or cross-linked polymers [14], and precursors of ceramic thin films [15]. The reader is invited to refer to two outstanding reviews to have a complete picture of these uses [4,16].

Alkylamine boranes such as $nC_xH_{2x+1}NH_2BH_3$ (denoted AAB) are the simplest derivatives of AB where the NH_3 of AB is substituted by an alkylamine $nC_xH_{2x+1}NH_2$. The lightest AAB is methylamine borane $CH_3NH_2BH_3$. It was discovered in the same time as AB [17], together with the ethyl, *n*-propyl and *n*-butyl compounds [18]. In the recent years, methylamine borane has been considered as a potential hydrogen storage material [6], as well as monomer of polyaminoborane [19] and precursor of B-C-N thin film [20]. In comparison, the ethylamine and *n*-propylamine boranes have received very little attention [4,16]. The *n*-butylamine borane was found to dehydropolymerize into a high-molecular-weight polyaminoborane (405,000 g mol^{-1}) [21]. To our knowledge, *n*-pentylamine borane has not been reported yet. The *n*-hexylamine borane was studied as precursor of *N*-substituted borazines [22], and more recently as a high energy density AB-based fuel [23]. Recently, we initiated a new work dealing with new AABs, one of the first being made of the *n*-dodecyl chain $nC_{12}H_{25}$. We expected that the addition of BH_3 to $nC_{12}H_{25}NH_2$ would lead to occurrence of dihydrogen $H^{\delta+}\cdots H^{\delta-}$ bonds between the NH_2BH_3 groups.

Dihydrogen $H^{\delta+}\cdots H^{\delta-}$ bonding has a central role in the chemistry of amine boranes and, though applied in a limited way, they may be applied in molecular self-assembly [24]. It is with this goal in mind that we investigated the behavior of *n*-dodecylamine borane $nC_{12}H_{25}NH_2BH_3$ (denoted as C12AB). It is worth mentioning that *n*-dodecylamine $nC_{12}H_{25}NH_2$ (denoted as C12A) is known as a neutral surfactant, and it was recently reported to allow nanostructuration of sodium borohydride $NaBH_4$ thanks to the steric hindrance of the alkyl chain and the occurrence of dihydrogen $H^{\delta+}\cdots H^{\delta-}$ bonds between its NH_2 head and the BH_4 entities [25]. Herein, we focus on the synthesis, stability against hydrolysis, and self-assembly of the borane derivative C12AB dissolved in THF.

2. Materials and methods

We used the following chemicals: *n*-dodecylamine $nC_{12}H_{25}NH_2$ (≥99%, from Sigma-Aldrich; C12A), borane dimethyl sulfide complex $(CH_3)_2SBH_3$ (2.0 M in THF, from Sigma-Aldrich), anhydrous THF (≥99.9%, from Sigma-Aldrich), and THF-d8 (99.5%, water <0.05%, from Eurisotop).

We synthesized *n*-dodecylamine borane $nC_{12}H_{25}NH_2BH_3$ (C12AB) by Lewis acid-base reaction, more specifically by substitution of the ligand (a Lewis base) of the BH_3 complex:

$$(CH_3)_2SBH_3 + nC_{12}H_{25}NH_2 \rightarrow nC_{12}H_{25}NH_2BH_3 + (CH_3)_2S \quad (1)$$

Typically, 0.93 g of C12A was mixed with 2.625 mL of the $(CH_3)_2SBH_3$ solution (in molar excess of 5%) in a flask inside an argon-filled glove box (MBraun M200B, O_2 and H_2O < 0.1 ppm). The mixture was stirred for 24 h at 500 rpm, under argon atmosphere and at 22 °C. The THF and the by-product $(CH_3)_2S$ were removed under vacuum at ambient temperature. We recovered a white solid (1 g) and transferred it into the glove box.

We analyzed C12AB by ^{1}H NMR spectroscopy (Bruker Avance III HD 400 MHz, BBOF probe) as well as by ^{11}B NMR spectroscopy (Bruker Avance III 500 MHz, CP-BBO cryoprobe), by Raman spectroscopy (confocal microspectrometer Labram HR, Jobin-Yvon, calibration performed using a silicon wafer at the theoretical wavenumber 521 cm^{-1}, argon-krypton-ion laser beam with a wavelength of 647.1 nm, power of 20-100 mW), and by FTIR spectroscopy (IS50 Thermo Fisher Scientific, 64 scans, resolution of 4 cm^{-1}). In parallel, we performed geometry optimization, NMR calculations, and vibrational analysis by using the

Gaussian 09 software. We determined the molecular structure of C12AB by density functional theory (DFT) calculations. We used the gas phase geometry optimization of the Gibbs free energy using B3LYP hybrid density functional with 6-311(++)G(2d,p) basis set at 298.15 K.

We used the inverted-burette method to measure the volume of H_2 generated by hydrolysis of C12AB (100 mg). Typically, 100 mg of C12AB was transferred in Schlenk tube-like flask under argon atmosphere, and the flask was connected to an inverted burette filled with water colored in blue. We set the reaction temperature at 30 or 40 °C. The H_2 evolution started upon the injection of 5 mL of deionized water in the reactor. We followed the H_2 evolution for 1 h.

We measured the hydrodynamic size and polydispersity of the C12AB aggregates by using dynamic light scattering (DLS) at fixed scattering angle ($\theta = 90°$). We performed the light scattering experiments by using an Amtec-goniometer equipped with a green laser with wavelength $\lambda = 532.5$ nm. Here q is the scattering vector; it is given by $4\pi n\lambda^{-1}\sin(\theta/2)$, with n the solvent refractive index and θ the scattering angle. We performed the measurements at the same incident light intensity (the laser power was set at 70 mW).

SAXS-WAXS experiments were performed on a home-built SAXS camera at the Institut de Chimie Séparative de Marcoule (ICSM). The setup involves a molybdenum source delivering a 1 mm large circular beam of energy 17.4keV. Monochromation is performed using a Fox-2D multishell mirror, and collimation of the beam is achieved using 2 sets of "scatterless" slits, which turn out to be crucial for the quantification of weak scattering near the beam-stop, together with precise monitoring of the transmission of the sample and solvents used as reference. The scattering pattern is recorded using a MAR345 two dimensional imaging plate with typical durations of 1h. The measurements were performed in transmission geometry, in 2 mm glass capillaries.

3. Results and discussion

3.1. Molecular analysis of C12AB

C12A is a clear and colorless liquid, whereas C12AB is a white solid. We analyzed them by ^{1}H NMR spectroscopy (THF-d8, 25 °C):

- C12A (δ in ppm): 0.91 (3H, t, 6.7 Hz, CH_3), 1.3 (18H, s broad, CH_2), 1.39 (2H, m, 6.6 Hz, CH_2CH$_2$N), 2.58 (2H, t, 6.6 Hz, CH_2N).
- C12AB (δ in ppm): 0.5-2 (3H, m, BH_3), 0.91 (3H, t, 6.6 Hz, CH_3), 1.31 (18H, s broad, CH_2), 1.55 (2H, m, 7.3 Hz, CH_2CH$_2$N), 2.61 (2H, quint, 7.3 Hz, CH_2N), 3.91 (2H, s broad, NH_2).

These ^{1}H NMR data reveal three differences that proves the formation of a B–N bond, thus the production of C12AB [26]. Indeed, there is an additional shielded signal between 0.6 and 2 ppm due to the resonance of BH_3, the signal belonging to the beta CH_2 of C12AB is downfield (1.55 versus 1.39 ppm), and a singlet due to NH_2 bound to BH$_3$ has appeared at 3.91 ppm. We then determined the purity of C12AB as being higher than 99% (Eq. 1).

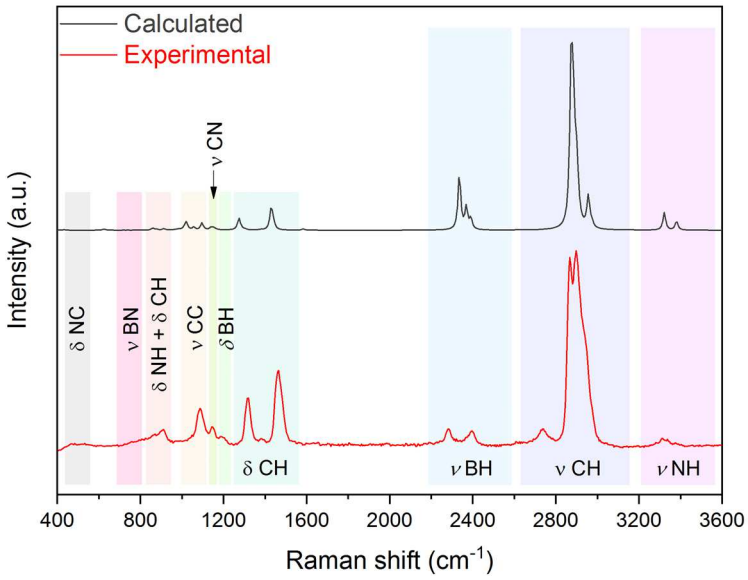

Figure 1. Raman spectrum of C12AB: experimental (bottom) and calculated (top).

We then analyzed the C12AB white solid by Raman and FTIR spectroscopy, and indexed each of the signals. The Raman spectrum (Figure 1) shows vibrational bands due to C–H, C–C, C–N, N–H, B–N, and B–H bonds [27,28], which is consistent with the molecular structure of C12AB. The Raman spectrum is besides consistent with the FTIR spectrum (Figure 2). Both spectra are in line with the elaboration of C12AB.

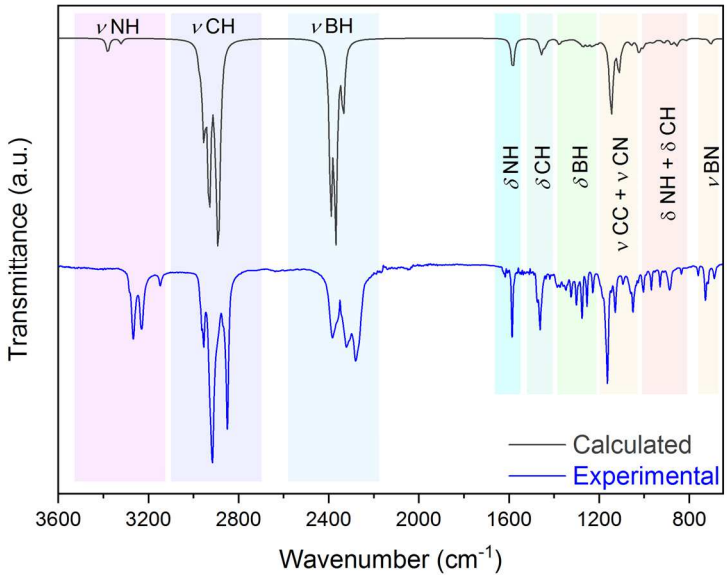

Figure 2. FTIR spectrum of C12AB: experimental (bottom) and calculated (top).

3.2. Stability of C12AB in solution

We studied the stability of C12AB (0.01 M) dissolved in THF-d8 by ^{11}B NMR spectroscopy. The analysis was undergone on the freshly prepared solution (Figure 3, curve labelled day 0). There is a single signal, a quartet located at δ −21 ppm ($^{1}J_{BH}$ 106 Hz) due to the resonance of BH_3 of C12AB, in good agreement with the calculated signal (δ −24.6 ppm, $^{1}J_{BH}$ 100 Hz). The solution was then kept sealed to be analyzed 1 day and 30 days afterwards (Figure 3). The spectrum recorded at day 1 shows the quartet of BH_3 at δ −19.2 ppm as well as two other signals of low intensity, a broad one at δ +20.4 ppm and another one at δ +1.5 ppm. These two additional signals are typical of borates, especially of tetrahedral BO_4 and trigonal BO_3 groups [29]. The signals were integrated, and the borates constitute 8% of the detected molecules. They much likely formed by hydrolysis of BH_3 because of the water (<0.05%) present in THF-d8. The hydrolysis has certainly occurred as follows:

$$n C_{12}H_{25}NH_2BH_3 + 3H_2O \rightarrow n C_{12}H_{25}NH_2 + B(OH)_3 + 3H_2 \quad (2)$$

$$n C_{12}H_{25}NH_2 + B(OH)_3 + H_2O \rightarrow n C_{12}H_{25}NH_3^+ + B(OH)_4^- \quad (3)$$

The spectrum recorded at day 30 is comparable to that recorded at day 1. The signals were integrated, and the borates still constitute 8% of the detected molecules. Further hydrolysis did not take place between day 1 and day 30. This indicates that C12AB is stable in THF.

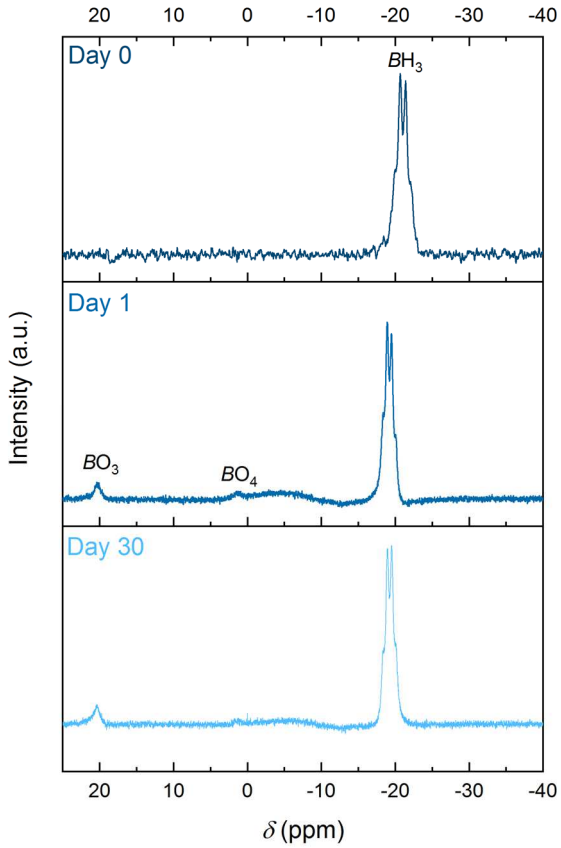

Figure 3. ^{11}B NMR spectra of C12AB (0.01 M) dissolved in THF-d8 (water content of <0.05%), recorded at day 0 (freshly prepared solution), day 1 and day 30.

We then repeated the experiments while adding some extra deionized water in order to have 3 equivalents of H_2O for 1 equivalent of C12AB (i.e. 1 H_2O per $H^{\delta-}$ of BH_3). Hydrolysis took place immediately, as evidenced by the ^{11}B NMR recorded shortly after the addition of H_2O into the C12AB solution (Figure 4). The singlet of high intensity located at δ +20 ppm is confirming the formation of $B(OH)_3$ by hydrolysis of C12AB (Eq. 3). This signal and the one due to BH_3 of C12AB at δ −19.5 ppm were integrated. $B(OH)_3$ was found to represent 25% of the detected molecules. The solution (kept sealed overnight) was analyzed again after 17 h. There is no difference between the two spectra, indicating that no change occurred. The signals were integrated, and $B(OH)_3$ still represents 25% of the detected molecules. Further hydrolysis did not take place.

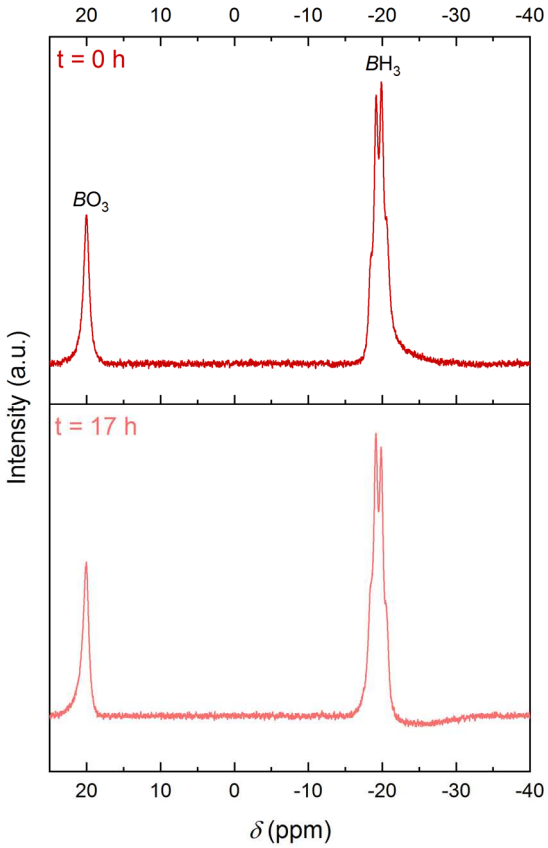

Figure 4. ^{11}B NMR spectra of C12AB (0.01 M) dissolved in THF-d8 and to which H_2O (0.03 M) was added, recorded a few moments after preparation and after 17 h.

C12AB is thus not stable in the presence of water. We verified this result by measuring the volume of H_2 generated when 1 equivalent of C12AB was put into contact with 553 equivalents of H_2O (i.e. 0.1 M C12AB). We performed a first experiment at 30 °C and a second one at 40 °C. The H_2 evolution curves (Figure 5) give rise to the following four observations. First, the hydrolysis starts immediately after C12AB has been into contact with H_2O. Second, the H_2 evolution follows a logarithmic-like growth: at 30 °C, the H_2 generation rate gradually decreases from 2.6 to <0.1 mL min^{-1}. Third, the conversion of C12AB is partial, being for example of 43% after 1 h of reaction at 30 °C. Fourth, the increase of the temperature improves both the kinetics of H_2 generation (e.g. with 3.3 mL min^{-1} at the beginning of the reaction) and the conversion after 1 h (50%). We then looked the vial containing the spent fuel recovered upon the reaction performed at 30 °C (inset picture in Figure 5). We witnessed two phases that consisted of the water and a hydrophobic solid (mixture of unreacted C12AB and the hydrolysis product C12A; Eq. 3), and we concluded that the hydrolysis reaction took place at the interface between the water surface and the

supernatant. This helped in understanding the reasons of the observations listed above. Finally, we analyzed a fraction of the water phase by ^{11}B NMR, which was done for the spent fuels obtained at 30 and 40 °C. The spectra (Figure 6) show only one signal at δ 19.1-19.3 ppm which is due to water-soluble $B(OH)_3$ (Eq. 3).

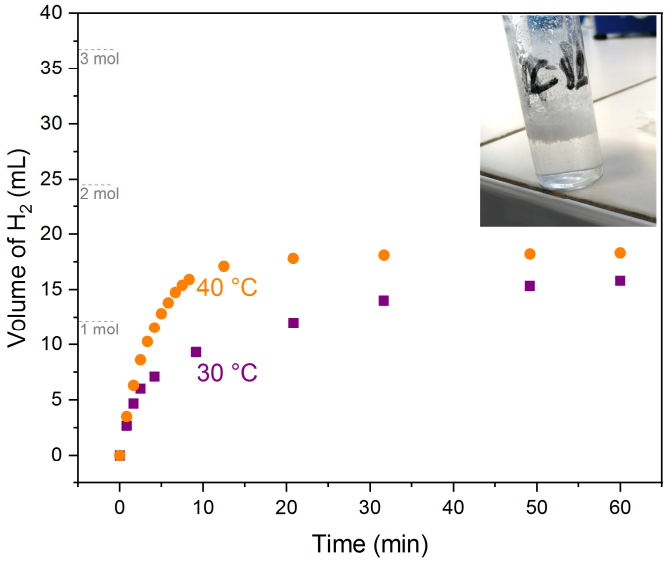

Figure 5. H_2 evolution curves for the hydrolysis of C12AB (0.1 M) in pure water performed at 30 (purple color) and 40 °C (orange color), over 1 h. The theoretical volumes corresponding to the release of 1, 2 and 3 moles of H_2 are indicated in the inside part of the left axis of the graph. The inset picture shows the vial containing the spent fuel recovered upon the reaction performed at 30 °C (100 mg C12AB in 5 mL H_2O), the spent fuel consisting of the water at the bottom of the vial and a supernatant white solid at the surface due to unreacted C12AB and C12A as product.

3.3. Self-assembly of C12AB in anhydrous THF

The dissolution of C12AB in anhydrous THF was studied by DLS. The mass concentration of C12AB was 1000 mg L^{-1}. The g_2-1 autocorrelation of C12AB as a function of the decay time τ, as well as that of C12A (for comparison), are shown in Figure 7. No autocorrelation was detected, indicating that C12AB and C12A, both with a mass concentration of 1000 mg L^{-1}, are well dissolved in THF. It is worth mentioning that DLS measurements at higher concentrations have not been possible due to the high turbidity of the solutions. Hence, the result obtained at 1000 mg L^{-1} represented a suitable starting point for further studies requiring the dissolution of C12AB in a good solvent like anhydrous THF.

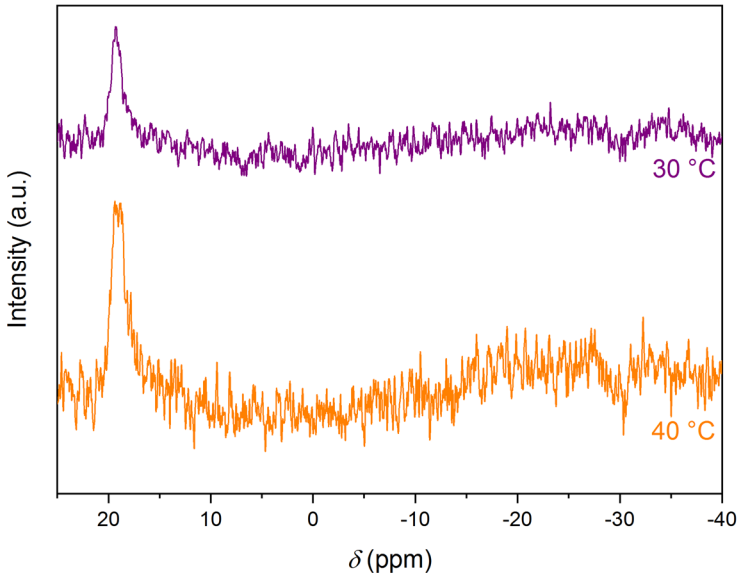

Figure 6. ^{11}B NMR spectra of the spent fuel (supernatant-free) after 1 h of hydrolysis of C12AB at 30 (purple color) and 40 °C (orange color), evidencing the formation of $B(OH)_3$ by hydrolysis.

We prepared five THF solutions of $C_{12}AB$ having mass concentrations of 0.1, 10, 25, 50 and 1000 mg L^{-1}. We then performed SAXS-WAXS experiments at room temperature (23 °C) in order to identify the concentration regime at which aggregates may form (Figure 8). The broad peak at high angles (q = 13.73 nm^{-1}) corresponds to the response of THF. Here, we have plotted the data in logarithmic scale to emphasize the regime between 0.1 and 5 nm^{-1}, where signals due to globular aggregates of typically 2 to 50 molecules form. Within this regime, there is an intensification of the signal with the increase of the mass concentration up to 1000 mg L^{-1}. Though the signal is weak, it can be attributed to small aggregates with a radius of 3 Å, as found with the help of the Guinier approximation (Figure 9). Since the electron density contrast between THF and the alkyl chain of the C12AB molecules is poor, we believe that the aggregates observed with X rays are due to the self-assembly of the NH_2BH_3 groups via dihydrogen $H^{\delta+}\cdots H^{\delta-}$ bonding. This result suggests that the C12AB molecules self-assemble into core-shell aggregates with the NH_2BH_3 groups in the core and the alkyl chain in an outer-shell. Considering the molecular volume of C12AB of 429 $Å^3$ and applying the Tanford formulae [30] to discriminate the molecular volumes of the C12AB's alkyl chain and NH_2BH_3 group (405 $Å^3$ and 24 $Å^3$ respectively), we estimated that each aggregate is formed with about five C12AB molecules (Figure 10). This core size R of 3 Å is also consistent with the estimated size of a fully stretched C12AB molecule with all-trans

conformation of 17 ± 1 Å. This is, to our knowledge, the first evidence of molecular self-assembly of an *n*-alkylamine borane dissolved in THF.

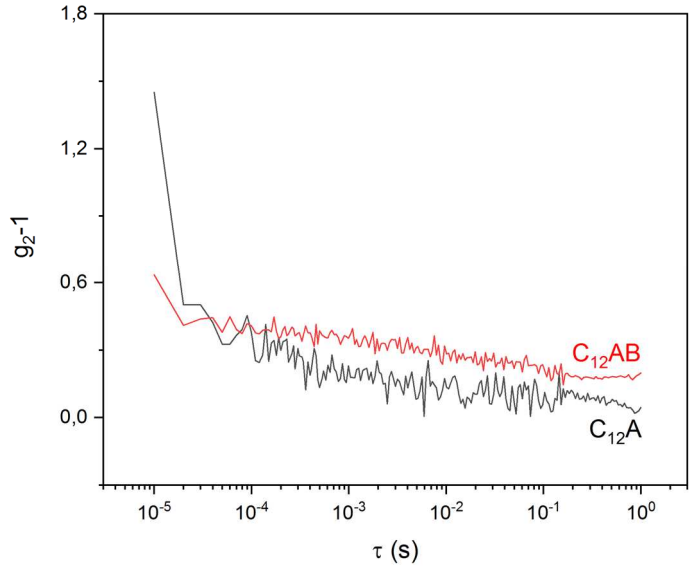

Figure 7. DLS measurements: signal from $C_{12}A$ (black color) and $C_{12}AB$ (1000 mg L^{-1} in anhydrous THF) (red color).

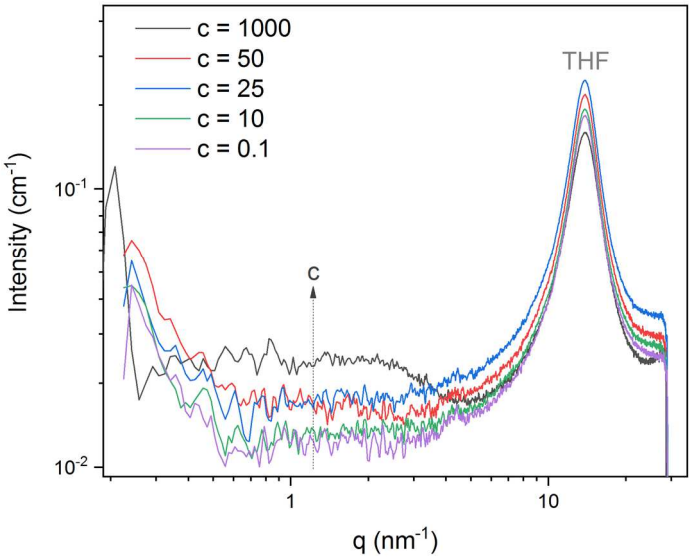

Figure 8. SAXS-WAXS measurements of $C_{12}AB$ in THF as a function of different concentrations (c = 0.1, 10, 25, 50 and 1000 mg L^{-1}); 23 °C.

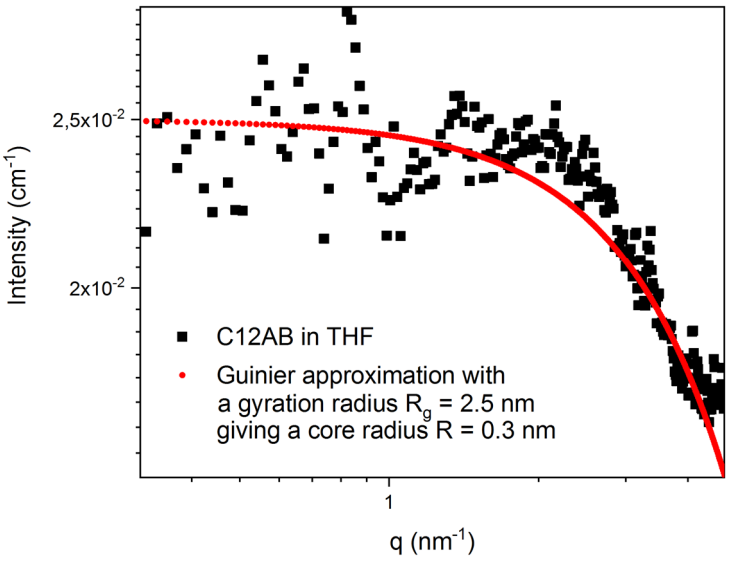

Figure 9. Guinier estimation of the radius formed by the self-assembled C12AB in THF.

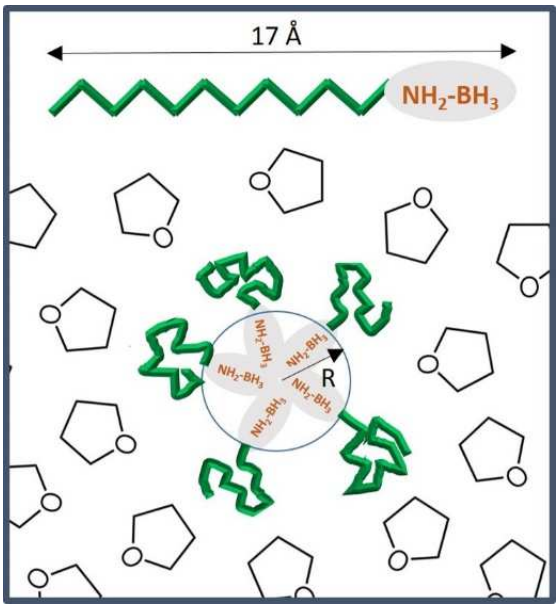

Figure 10. Illustration of the C12AB aggregates formed in THF.

4. Conclusion

As discussed above, we focused on the synthesis and characterization of C12AB as well as on its stability against hydrolysis and its dihydrogen $H^{\delta+}\cdots H^{\delta-}$ bonding-driven self-assembly. In a first step, C12AB, a white solid, was synthesized by Lewis acid-base reaction involving

$(CH_3)_2SBH_3$ in anhydrous THF and the colorless liquid-state C12A, under argon and at 22 °C. C12AB was produced with a purity higher than 99%. In a second step, the stability of C12AB dissolved in THF was studied. It is stable unless the solvent contains moisture. It indeed reacts with H_2O by hydrolysis, resulting in the formation of water-soluble borates. C12AB has thus to be stored and handled in anhydrous conditions. In a third step, we investigated the formation of aggregates by self-assembly of C12AB in anhydrous THF which is a good solvent of it. Core-shell aggregates form. They consist of about five self-assembling stretched C12AB molecules where the NH_2BH_3 groups are in the core of 3 Å and the alkyl chains in an outer-shell. In conclusion, our results evidence the occurrence of dihydrogen $H^{\delta+}\cdots H^{\delta-}$ bonding between the C12AB molecules in anhydrous THF towards the formation of core-shell aggregates. This could be applied to the synthesis of advanced nanostructured materials [24]. Works are in progress.

Acknowledgments

We thank the Agence Nationale de la Recherche for funding: ANR-10-LABX-05-01 (LabEx CheMISyst in the frame of the program "Investissement d'Avenir"), and ANR-18-CE05-0032 (project REVERSIBLE). UBD thanks Dr. Jean-Fabien Petit (2012-2015) and Dr. Salem Ould-Amara (2017-2017) who performed the preliminary experiments leading to the aforementioned projects and the present work.

References

[1] J.L. Gay-Lussac, J.L. Thenard, Des propriétés de l'acide fluorique et surtout de son action sur le métal de la potasse, Mem. Phys. Chim. Soc. D'Arcueil 2 (1809) 317-331.

[2] A.B. Burg, H.I. Schlesinger, Hydrides of boron. VII. Evidence of the transitory existence of borine (BH_3): Borine carbonyl and borine trimethylammine, J. Am. Chem. Soc. 59 (1937) 780-787.

[3] S.G. Shore, R.W. Parry, The crystalline compound ammonia-borane, H_3NBH_3, J. Am. Chem. Soc. 77 (1955) 6084-6085.

[4] A. Staubitz, A.P.M. Robertson, M.E. Sloan, I. Manners, Amine- and phosphine-borane adducts: New interest in old molecules, Chem. Rev. 110 (2010) 4023-4078.

[5] R. Kumar, A. Karkamkar, M. Bowden, T. Autrey, Solid-state hydrogen rich boron–nitrogen compounds for energy storage, Chem. Soc. Rev. 48 (2019) 5350-5380.

[6] L. Luconi, G. Tuci, G. Giambastiani, A. Rossin, M. Peruzzini, H_2 production from lightweight inorganic hydrides catalyzed by 3d transition metals, Int. J. Hydrogen Energy 44 (2019) 25746-25776.

[7] L. Zhang, S. Li, Y. Tan, Z. Tang, Z. Guo, X. Yu, Synthesis and hydrogen release properties of alkyl-substituted amine-boranes, J. Mater. Chem. A 2 (2014) 10682-10687.

[8] W. Luo, L. N. Zakharov, S. Y. Liu, 1,2-BN cyclohexane: Synthesis, structure, dynamics, and Reactivity, J. Am. Chem. Soc. 133 (2011) 13006-13609.

[9] J. Tao, N. Lv, L. Wen, Y. Qi, X. Lv, Hydrogen release mechanisms in $LiNH_2BH_3{\cdot}NH_3BH_3$: A theoretical study, J. Mol. Struct. 1081 (2015) 437-442.

[10] B.S. Burnham, Synthesis and pharmacological activities of amine-boranes, Curr. Med. Chem. 12 (2005) 1995-2010.

[11] A. Flores-Parra, R. Contreras, Boron coordination compounds derived from organic molecules of biological interest, Coord. Chem. Rev. 196 (2000) 85-124.

[12] P.V. Ramachandran, A.S. Kulkarni, Y. Zhao, J. Mei, Amine–boranes bearing borane-incompatible functionalities: application to selective amine protection and surface functionalization, Chem. Commun. 52 (2016) 11885-11888.

[13] G.C. Andrews, Chemoselectivity in the reduction of aldehydes and ketones with amine boranes, Tetrahedron Lett. 21 (1980) 697-700.

[14] N.E. Stubbs, A.P.M. Robertson, E.M. Leitao, I. Manners, Amine–borane dehydrogenation chemistry: Metal-free hydrogen transfer, new catalysts and mechanisms, and the synthesis of polyaminoboranes, J. Organomet. Chem. 730 (2013) 84-89.

[15] R.Y. Tay, H. Li, S.H. Tsang, M. Zhu, M. Loeblein, L. Jing, F.N. Leong, E.H.T. Teo, Trimethylamine borane: A new single-source precursor for monolayer h-BN single crystals and h-BCN thin films, Chem. Mater. 28 (2016) 2180-2190.

[16] B. Carboni, L. Monnier, Recent developments in the chemistry of amine- and phosphine-boranes, Tetrahedron 55 (1999) 1197-1248.

[17] T.C. Bissot, R.W. Parry, Preparation and properties of trimeric N-methylaminoborane, J. Am. Chem. Soc. 77 (1955) 3481-3482.

[18] M.P. Brown, R.W. Heseltine, D.W. Johnson, Studies of aminoboranes. Part I. Reactions involving transfer of hydrogen from N-monoalkyl-substituted aminoboranes and amine–boranes to dimethylaminoborane, J. Chem. Soc. A (1967) 597-601.

[19] F. Anke, D. Han, M. Klahn, A. Spannenberg, T. Beweries, Formation of high-molecular weight polyaminoborane by Fe hydride catalysed dehydrocoupling of methylamine borane, Dalton Trans. 46 (2017) 6843-6847.

[20] F. Leardini, E. Flores, A.R. Galvis, I.J. Ferrer, J.R. Ares, C. Sánchez, P. Molina, H.P. van der Meulen, C.G. Navarro, G. López Polin, F.J. Urbanos, D. Granados, F.J. García-García, U.B. Demirci, P.G. Yot, F. Mastrangelo, M.G. Betti, C. Mariani, 2018. Nanotechnology. 29, 025603.

[21] A. Staubitz, A.P. Soto, I. Manners, Iridium-catalyzed dehydrocoupling of primary amine–borane adducts: a route to high molecular weight polyaminoboranes, boron–nitrogen analogues of polyolefins, Angew. Chem. 120 (2008) 6308-6311.

[22] E. Framery, M. Vaultier, Efficient synthesis and NMR data of N- or B-substituted borazines, Heteroatom Chem. 11 (2000) 218-225.

[23] A.E. Carre-Burritt, B.L. Davis, B.D. Rekken, N. Mack, T.A. Semelsberger, Enabling ammonia-borane: co-oligomerization of ammonia-borane and amine-boranes yield liquid products, Energy Environ. Sci. 7 (2014) 1653-1656.

[24] X. Chen, J.C. Zhao, S.G. Shore, The roles of dihydrogen bonds in amine borane chemistry, Acc. Chem. Res. 46 (2013) 2666-2675.

[25] T. Wang, K.F. Aguey-Zinsou, Controlling the growth of $NaBH_4$ nanoparticles for hydrogen storage, Int. J. Hydrogen Energy 45 (2020) 2054-2067.

[26] A. Flores-Parra, C. Guadarrama-Pérez, J.C.G. Ruiz, S.A.S. Ruiz, G.V. Suarez-Moreno, R. Contreras, Mono- and di-alkyl-[1,3,5]-dithiazinanes and their N–borane adducts revisited. Structural and theoretical study, J. Mol. Struct. 1047 (2013) 149-159.

[27] B. La Serna, M. Hernandez, J.H. Bertran, On the conformation of the five-membered ring of dipropyl(γ-amino propyl)borane, J. Mol. Struct. 95 (1982) 271-272.

[28] J.R. Durig, N.E. Lindsay, T.J. Hizer, J.D. Odom, Infrared and raman spectra, conformational stability and normal coordinate analysis of ethyldimethylamine-borane, J. Mol. Struct. 189 (1988) 257-277.

[29] H. Nöth, H. Vahrenkamp, Kernresonanzuntersuchungen an Bor-Verbindungen, I. ^{11}B-Kernresonanzspektren von Boranen mit Substituenten aus der ersten Achterperiode des Periodensystems, Chem. Ber. 99 (1966) 1049-1067.

[30] C. Tanford, Micelle shape and size, J. Phys. Chem. 76 (1972) 3020-3024.